Journal of
Composites Science

MDPI

Article

Gypsum–Cement–Pozzolan Composites for 3D Printing: Properties and Life Cycle Assessment

Genadijs Sahmenko [1], Liga Puzule [1], Alise Sapata [2], Peteris Slosbergs [2], Girts Bumanis [1], Maris Sinka [2,*] and Diana Bajare [1]

[1] Institute of Sustainable Building Materials and Engineering Systems, Faculty of Civil and Mechanical Engineering, Riga Technical University, LV-1658 Riga, Latvia; genadijs.sahmenko@rtu.lv (G.S.); liga.puzule@rtu.lv (L.P.); girts.bumanis@rtu.lv (G.B.); diana.bajare@rtu.lv (D.B.)
[2] 3D Concrete Printing Laboratory, Institute of Sustainable Building Materials and Engineering Systems, Faculty of Civil and Mechanical Engineering, Riga Technical University, LV-1658 Riga, Latvia; alise.sapata@rtu.lv (A.S.); peteris.slosbergs@rtu.lv (P.S.)
* Correspondence: maris.sinka@rtu.lv

Abstract: Over the past decade, 3D printing with concrete has been widely adopted worldwide. The primary drivers for this innovation are the reduction in manual labor and the more efficient use of natural resources. New materials that are suitable for 3D printing are developed, which are characterized by rapid setting and robust physical and mechanical properties. In this study, for the first time, ternary gypsum–cement–pozzolanic (GCP) composites were developed and evaluated for use in 3D printing. These composites are associated with durability in water as Portland cement (PC) while maintaining the rapid hardening properties of gypsum. Two types of secondary gypsum—recycled plasterboard gypsum (RG) and phosphogypsum (PG)—were used as the calcium hemihydrate component. The compressive strength test showed that 37 MPa can be achieved, which is comparable to that of traditional PC-based 3D printable mixtures. For the first time in a 3D print test, it was experimentally proved that GCP mixtures have good stability and buildability up to 35 layers. According to Life Cycle Analysis, elaborated material gives a carbon footprint reduction of up to 40%, compared to traditional PC mortar, thus supporting the sustainable use of this innovative composite.

Keywords: concrete 3D printing; gypsum–cement–pozzolan (GCP); recycling; secondary gypsum; phosphogypsum; carbon footprint; Life Cycle Analysis (LCA)

Citation: Sahmenko, G.; Puzule, L.; Sapata, A.; Slosbergs, P.; Bumanis, G.; Sinka, M.; Bajare, D. Gypsum–Cement–Pozzolan Composites for 3D Printing: Properties and Life Cycle Assessment. *J. Compos. Sci.* **2024**, *8*, 212. https://doi.org/10.3390/jcs8060212

Academic Editor: Francesco Tornabene

Received: 26 April 2024
Revised: 22 May 2024
Accepted: 4 June 2024
Published: 6 June 2024

1. Introduction

The construction sector reportedly produces 33% of the world's greenhouse gas emissions (GHG) [1]. Consequently, more studies are focused on developing strategies to reduce these emissions by replacing energy-consuming building materials with more sustainable and environmentally friendly alternatives. Portland cement (PC) is identified as the main source of CO_2 and energy emissions in the construction industry. According to data from the International Energy Agency, 7% of global CO_2 emissions are associated with PC production. Many studies have already investigated the use of well-known PC with supplementary cementitious materials, varying in efficiency and replacement intensity [2]. On the other hand, gypsum is known as a widely available and low-carbon-footprint material, emitting at least five times less CO_2 compared to PC [3,4]. However, the disadvantage of gypsum binder is its low water resistance and relatively low strength.

A logical development of binder selection would be the combination of PC and gypsum (Ref. [5]). Calcium sulphoaluminate cement–ordinary Portland cement (OPC)–gypsum with around 80% OPC and 10% gypsum is reported to reach 24 MPa strength, while hardening is provided by the formation of ettringite, leading to a slight expansion effect [6]. It is well known that gypsum content above 7% in the OPC can lead to deleterious expansion reactions due to the formation of ettringite [7]. To avoid uncontrolled crystallization of

ettringite, pozzolanic materials are incorporated into the mixture, and a ternary system binder called gypsum–cement–pozzolan (GCP) is obtained [8,9].

In contrast to gypsum, ternary GCP composition is an alternative binder that is water-resistant and makes it possible to obtain much higher mechanical strength that can approach the strength of a PC binder. Moreover, combining gypsum with pozzolan and PC in a ternary composite is reported to enhance the initially low green strength typically associated with pure gypsum. GCP binders have significant potential in the development of early strength and are distinguished from pure gypsum binding materials by their capacity for hydraulic hardening and improved water resistance [10]. Furthermore, GCP, in terms of environmental friendliness, is much closer to gypsum, as more than 50% of the binder is based on gypsum. In the research [11], the authors performed LCA for different alternative binding systems, noting the promising outlook for using a ternary system binder based on the GCP system.

The ternary concept of mixture enables the use of not only conventional raw materials but also various industrial wastes and by-products, for instance, secondary gypsum obtained from processing waste plasterboard sheets—recycled gypsum (RG) [12]—and an artificial gypsum by-product, phosphogypsum (PG), which is created as a by-product from mineral fertilizer production [13]. Gypsum content in the RG can vary from 38% to 92% depending on its source, and strength of up to 4 MPa is reported. Such strength is not satisfactory for its application alone, while in ternary GCP compositions, the strength could be significantly improved.

In the past decade, alternative strategies to save resources have been developed by scientists, universities, and companies through the formulation of compositions and technologies for concrete 3D printing [14–17]. Numerous advantages are showcased by 3D printing technology over conventional concrete construction methods, such as casting. The potential to reduce costs by up to 80%, decrease material consumption by 30–60%, minimize construction waste by up to 60%, and increase production efficiency by up to 70% has been recognized [18,19]. Given these benefits, the exploration of new construction materials suitable for 3D printing is considered crucial.

Traditionally, PC-based compositions are regarded as most suitable for 3D printing. Nevertheless, gypsum has also a longstanding history in 3D printing, with demonstrated adaptability and compatibility with the process [20–22]. In 3D printing, the vastly used gypsum typically exists in the form of α-hemihydrate gypsum (α-HG). The morphology of α-HG powder, which features large, dense, and substantial crystals, is noted to improve workability in 3D printing. These characteristics are found to facilitate smoother flow and deposition during the printing process, resulting in enhanced handling and precision [21,22]. The rapid setting time characteristic of gypsum is helpful in improving the stability and buildability of 3D-printed structures. Typically, α-HG with the particle shape suited for 3D printing is obtained from raw gypsum. However, recent studies have shown that α-HG with controlled morphology can be obtained from RG [21,22] and by recycling industrial by-products such as PG [23,24].

Despite recent progress in incorporating RG into 3D printing, challenges are encountered in achieving optimal printability and homogeneity due to its tendency to agglomerate. This issue is attributed to the high hygroscopicity and water reactivity of waste gypsum particles [21].

The existing research shows that due to its favorable morphology, α-hemihydrate gypsum exhibits higher mechanical properties in comparison to β-hemihydrate gypsum. However, the manufacturing process of α-hemihydrate gypsum is costly and limits its usage on a large scale [25,26]. As previously mentioned, extensive research has been conducted on the use of α-hemihydrate gypsum in 3D printing. However, there is a notable deficiency in studies focusing on the utilization of β-hemihydrate gypsum in 3D printing.

It should be noted that when summarizing the literature, there is almost no information on the use of trinary GCP compositions in 3D printing, as well as a lack of research on the LCA of this type of composition. To verify the reduced environmental impact GCP can

provide, LCA is considered a great tool to validate sustainability [27,28]. There is related research on the application of adobe reinforced with cement–gypsum–lime in 3D printing technology, and the results show that increasing the amount of gypsum and lowering the amount of PC show less impact on the environment [29]. Similar studies show that encouraging outcomes have emerged from ternary systems comprising gypsum, lime, and pozzolan. Typically, these systems offer a reduced carbon footprint compared to those incorporating PC [30]. Although gypsum already shows high potential, when developing new construction materials, it can be improved when changed to RG. To preserve natural gypsum deposits and repurpose large quantities of waste by-products, gypsum recovered from construction demolition waste could be re-used for new construction materials [31].

Also, GCP has been researched before, but the application of GCP in 3D printing has not been performed. For the first time, we aim to research set time adaptation and description of the buildability of the GCP mixture. The LCA analysis of GCP will support the development of green building practice for 3D printable materials.

2. Materials and Methods

2.1. Raw Materials

Ordinary Portland cement CEM I 42.5N (Schwenk Ltd., Broceni, Latvia) in accordance with EN 197-1 [32] was used for experimental mix preparation. In accordance with producer's data, the cement had fineness of 350 m^2/kg (by Blaine), density of 3.16 g/cm^3, and setting time of 180 min. Compressive strength on 2nd day—24 MPa, on 7th day—39 MPa, and on 28th day—51 MPa. Although more sustainable types of cement have replaced CEM I in some areas, this study specifically used CEM I to more accurately observe the interactions between gypsum, cement, and pozzolan. This approach will serve as a basis for future development of GCP recipes using different types of cement.

Three types of gypsum were used. Gypsum plaster/building gypsum β-hemihydrate gypsum Baugips (Knauf Ltd., Sauriesi, Latvia) (BG) was applied as reference gypsum (conforming to the standard EN 13279-1 [33]). The set time is noted to be from 10 to 12 min, and the compressive strength exceeds 6 MPa.

The second type of gypsum binder is a secondary gypsum that was recovered from the waste of plasterboard sheets (RG). The technological process for obtaining RG binder is shown in Figure 1. The initial technological step involved collecting plasterboard sheets from construction site, its classification, and separation (Figure 1a). Then, the raw material was thermally treated at a temperature of 140 °C in laboratory thermal chamber (Figure 2b,c). Subsequent operations included the separation of cardboard and crushing of the gypsum material in jaw crusher (Figure 1d) to obtain particle mix < 12 mm (Figure 1e). Disintegrator Desi-15 (50 Hz, 3000 rpm) was used for material collision milling (Figure 1f). The milling occurs due to the impact of particles on the disk rods that rotate in opposite directions (Figure 1g). The result was a powdered gypsum binder RG (Figure 1h). The properties of RG were previously described by the authors [12]. Compared to BG, RG was characterized by smaller grains and a more porous particle microstructure (Figure 2a,b).

The third type, dihydrate phosphogypsum (PG), was obtained from AB Lifosa (Kedaini, Lithuania) where PG is generated as a waste coming from fertilizer production. It was fired at 140 °C and milled in a disintegrator to produce a gypsum by-product binder [18]. Microstructural image obtained with SEM shows quite dense microstructure of the PG particle (Figure 2c). Visually, PG particles have a denser microstructure compared to RG particle (Figure 2b).

A pozzolanic component is a mandatory part of the GCP composition. In this case, high-reactivity metakaolin (MK) was utilized as the pozzolanic component, providing chemical stability to the GCP system. MK was produced by the dehydration of kaolin clay mineral ($Al_2(OH)_4Si_2O_5$). MK, a highly reactive alumino-silicate compound, was transformed into a dehydrated and amorphous state with a chemical formula of $Al_2Si_2O_7$ after the firing process, which occurred at temperatures ranging from 700 to 800 °C. In this study, commercially available MK, obtained from Astra Polska company, was used.

According to SEM images (Figure 2d), MK particles were observed to have much smaller sizes compared to gypsum particles. Thus, more effective microstructural packing of the binder paste in the GCP was anticipated, in comparison to mono-component binders (such as PC or gypsum binders).

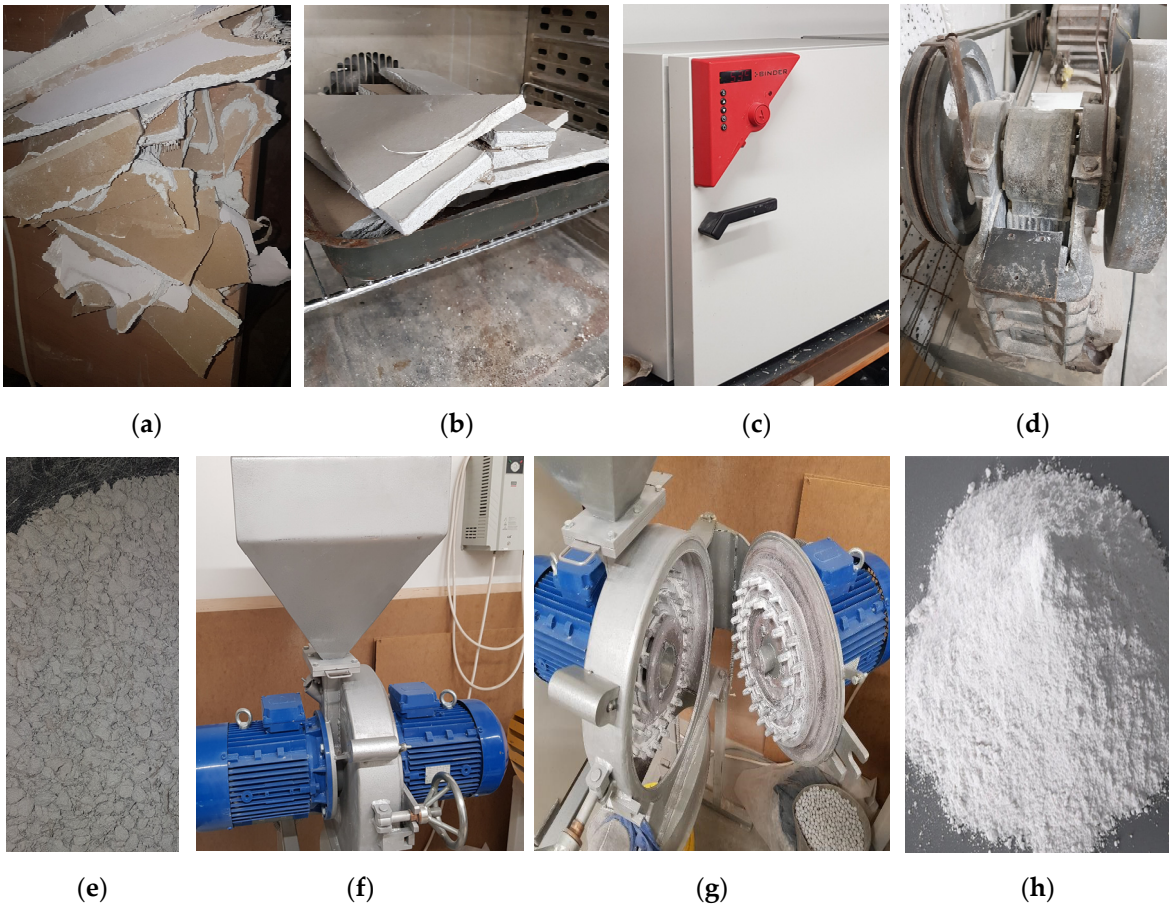

Figure 1. Used gypsum board recycling process to obtain secondary gypsum binder (RG): (**a**) collection of gypsum plasterboard; (**b**,**c**) thermal treatment (140–145 °C, 4 h); (**d**) crushing with laboratory jaw crusher; (**e**) roughly crushed gypsum (<11.2 mm) prepared for milling; (**f**) collision milling in disintegrator Desi-15 (50 Hz, 3000 rpm); (**g**) intensive milling occurs due to the impact of particles on the disk rods which rotate in opposite directions; (**h**) prepared RG binder for the use in GCP.

To make binder suitable for 3D printing, two filling materials were used: limestone powdered filler (Saulkalne Ltd., Saulkalne, Latvia) and washed commercial sand 0/2 mm (Sakret Ltd., Rumbula, Latvia).

The particle size grading of the binding components and fillers used is shown in the diagram in Figure 3. PC, limestone filler, and MK were identified as having the finest particle size distribution. Particle size analysis of these materials was performed using the laser diffraction method. Sand was identified as the coarsest filling material in the tested mixes, with particle sizes up to 2 mm. The granulometric curves of the three types of gypsum are positioned between the sand and PC. The data from the particle size analysis are consistent with the SEM image results and the information provided by the manufacturers of PC and MK.

Admixtures were used to control the setting time of the mixtures and ensure necessary workability. The mix based on PC was prepared by Sakret Ltd. (Rumbula, Latvia) using a complex admixture consisting of a plasticizing agent and a viscosity-modifying component. For GCP mixtures, a complex retarding and water-reducing admixture *Plastretard* was used (provided by Knauf Ltd., Saurieši, Latvia).

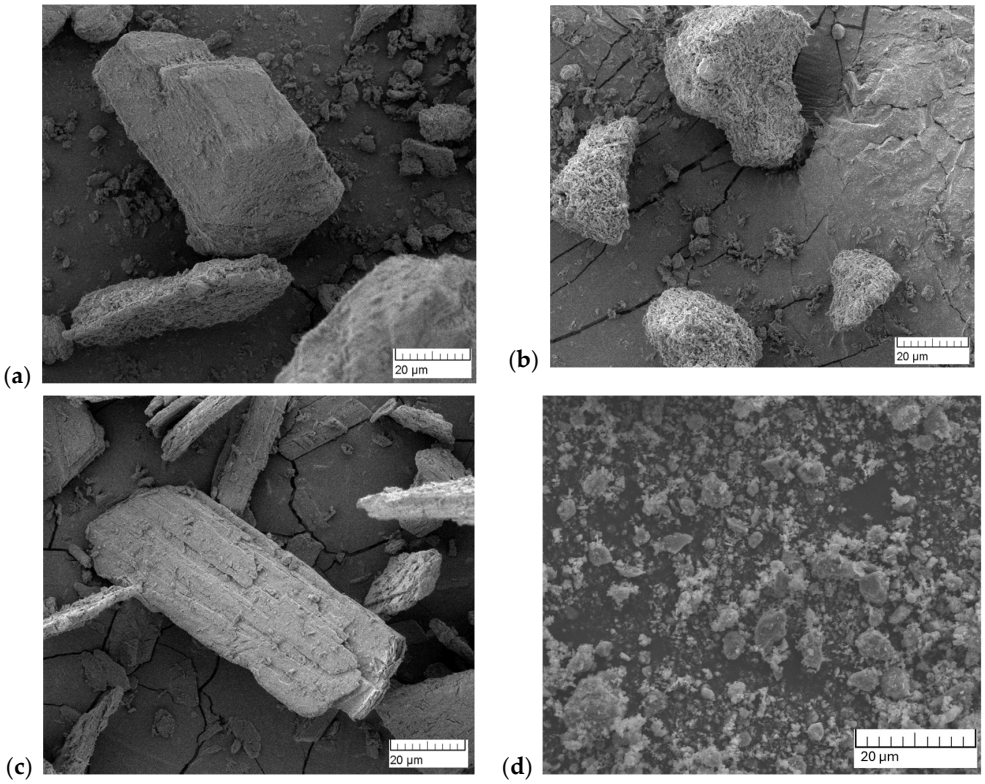

Figure 2. SEM images: (**a**) building gypsum (BG); (**b**) recycled board gypsum, thermally treated (RG); (**c**) phosphogypsum, thermally treated (PG); (**d**) metakaolin powder (MK).

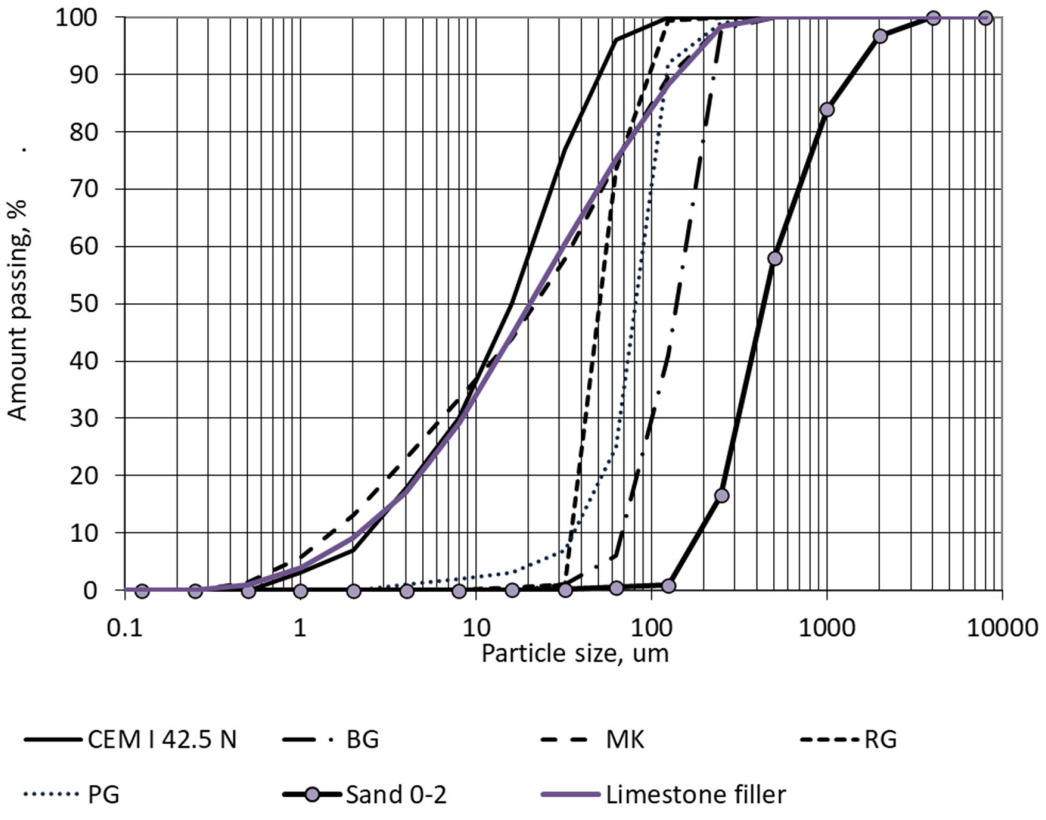

Figure 3. The particle size distribution of raw materials for GCP.

2.2. Mix Preparation

In this study, six mixture formulations were prepared. The reference mix "PC mortar" based on PC, sand, and limestone filler is a commercial material used for concrete 3D printing technologies developed by Sakret Ltd. (Latvia). GCP experimental mixes GCP1, GCP2, GCP3, GCP4, and GCP5 were composed of gypsum–cement–pozzolan. In trial experiments, GCP mixes were developed and optimized with the aim of achieving the best mechanical properties and water resistance of the material. In the compositions of GCP, major part of binder constituting 55% by mass was gypsum, while PC and MK each accounted for 22.5%.

Mix GCP1 served as the reference composition, based on BG. In mix GCP2, half of the BG was replaced with RG. In mix GCP3, all gypsum components of the composition were replaced with RG. The composition for GCP4 was based on PG. Formulation GCP5 was created using a combination of PG and RG in a 1:1 ratio.

The purpose of the admixtures was to plasticize the mix, reduce the water–binder ratio, and provide the necessary stability and printability. Section 2.4 provides a more detailed description of determining the required amount of water to achieve a printable mixture. The weight proportions of the mixture compositions are summarized in Table 1. Binder-to-sand ratio in GCP mixtures was used as 1:0.5 to ensure good printing properties, although the amount of sand could be increased in the future. Binder-to-filler ratio for PC mortar had been previously optimized by the producer to ensure effective use of the binder. The proportions between gypsum component, PC, and MK remained the same in all mixtures.

Table 1. Experimental mix compositions (wt. proportions).

Mix No.:	PC Mortar	GCP1	GCP2	GCP3	GCP4	GCP5
Building gypsum (BG)	-	0.550	0.275	-	-	-
Recycled gypsum (RG)	-	-	0.275	0.550	-	0.275
Phosphogypsum (PG)	-	-	-	-	0.550	0.275
CEM I 42.5 N	1.000	0.225	0.225	0.225	0.225	0.225
Metakaolin (MK)	-	0.225	0.225	0.225	0.225	0.225
Limestone filler	0.670	-	-	-	-	-
Water	0.500	0.460	0.540	0.620	0.530	0.600
Admixture *Plastretard*	-	0.005	0.005	0.005	0.005	0.005
Complex admixture	0.033	-	-	-	-	-
Sand 0/2 mm	1.600	0.500	0.500	0.500	0.500	0.500

The sequence of preparing the mixtures was as follows. Dry components were dosed with an accuracy of ±1% and pre-mixed. Additives were previously dissolved in water. Then, while mixing, water with admixtures was added to ensure the necessary mix workability. A mixing time of 3 min was used.

2.3. Sample Testing

To test the physical and mechanical properties, cube samples with a side of 20 mm were produced, 15 for each series. During the first 24 h after casting, the samples were kept in molds covered with plastic film. Subsequently, after demolding, the samples underwent hardening. The curing of the samples was conducted under conditions of normal temperature (20–22 °C) and air relative humidity of 95 ± 5%.

Strength and density were determined under specified moisture conditions of the materials: in the wet state after normal curing (f_{wet}) and in the dry state after drying (f_{dry}) at 50 °C for 24 h before testing. Prior to testing, the samples were weighed and measured to determine the material's density. Compressive strength was determined using a universal testing machine with a capacity of 20 kN. During the compression test, the samples were loaded at a rate of 1.0 mm/min. Sample destruction took place from 30 to 60 s, which corresponds to a loading rate of approximately 1.2–1.5 MPa/s. This value corresponds

to the standard for testing cement samples EN 196-1 [34], which defines loading rate of 1.5 ± 0.125 MPa/s (clause 9.2).

The water absorption of the material (W) was determined by calculating the ratio of the mass of absorbed moisture to the mass of the dry sample:

$$W = (m_{wet} - m_{dry})/m_{dry} \times 100\% \quad (1)$$

Strength testing was conducted at the ages of 7 and 28 days. At 28 days, samples were tested both in a water-saturated state and after drying. This method facilitated the determination of the water absorption of the material as well as the softening coefficient (K), which is defined as the ratio of the strength in a water-saturated state to the strength in a dry state. The softening coefficient is calculated as the ratio of the strength in the wet state f_{wet} to the strength in the dry state f_{dry}:

$$K = f_{wet}/f_{dry} \quad (2)$$

2.4. Evaluation of Material's Suitability for 3D Printing

The flow table consistency test according to EN 1015-3 [35] was chosen to assess the suitability for 3D printing due to its efficiency and its ability to quickly determine material consistency without requiring large quantities of material. This method is recognized by researchers specializing in additive manufacturing as a simple approach to describing workability and the properties of fresh material [36,37]. See Section 3.3 for the consistency results and suitability for 3D printing of each mixture.

Buildability, another parameter for evaluating a material's suitability for 3D printing, is defined as the ability of a material to retain its shape and stability after several layers have been deposited onto each other, resulting in an increasing load [38–40]. Although buildability can be assessed using various indirect test methods [36], in this case, it was decided to measure it directly through 3D printing.

3D printing for buildability assessment was carried out for one of the mixtures. The mixture was prepared by first homogenizing all dry ingredients through mixing. Meanwhile, the setting retarder was dissolved in water. Water solution was then added to the dry mixture and mixed for 180 s. A total of 25 liters of mass was mixed using a portable mortar mixer, RUBIMIX-9N, operating at a speed of 780 RPM. Immediately after mixing, the mixture was loaded into the printer. Printing was performed using a gantry-type printer with a batch-type printhead developed within RTU 3D Concrete Printing Laboratory [41]. The printer frame allows for print region dimensions of $1500 \times 1000 \times 1000$ mm.

To assess buildability, two print objects—a straight wall and a square-shaped object measuring 500 mm and 200×200 mm, respectively—were printed. Both objects were printed simultaneously with a layer interval time of 26 s. The targeted print object height was 30 layers, with one layer height of 10mm, completing the printing in 15 min.

2.5. Life Cycle Assessment

The life cycle inventory is displayed in Table 2, including all data from the Ecoinvent database. Modifications were made to three of the processes—recycled gypsum, phosphogypsum, and metakaolin—since these materials are not available in the Ecoinvent database.

As previously mentioned, the recycled gypsum originates from gypsum plasterboards; therefore, the gypsum plasterboard process was taken and modified. Transport data were derived from the gypsum plasterboard market process, and data for water and energy were taken from the transformation process, as the raw material was recycled.

Similarly, the PG process was devised. In this case, the process for gypsum as a mineral was additionally used, incorporating impacts from stockpiled PG [42]. Transport data were utilized from the market process, and land occupation and emissions data were taken from the transformation process. As this is a preliminary LCA to generally assess the impact of GCP, further research is needed to develop both of these gypsum products further, to obtain more precise results.

Table 2. Life cycle inventory for 1 kg of each material used in the composition.

Material	Amount	Unit	Data from Ecoinvent or Modified
Baugips Knauf (BG)	1	kg	Stucco {GLO} | market for | Cut-off, U
Recycled gypsum (RG)			Gypsum, mineral {CH} | gypsum quarry operation | Cut-off, U (modified); Gypsum plasterboard {RoW} | production | Cut-off, U (modified)
Phosphogypsum (PG)	1	kg	Gypsum, mineral {RER} | market for gypsum, mineral | Cut-off, U (modified); Gypsum, mineral {CH} | gypsum quarry operation | Cut-off, U (modified)
CEM I 42.5 N	1	kg	Cement, limestone 6–10% {RoW} | market for cement, limestone 6–10% | Cut-off, U
Metakaolin [30]	1.14	kg	Kaolin {GLO} | market for | Cut-off, U
	2.14	MJ	Heat, district or industrial, other than natural gas RoW} | market for | Cut-off, U
Limestone filler	1	kg	Supplementary cementitious materials {RER} | limestone, crushed, washed to generic market for supplementary cementitious materials | Conseq, U
Water	1	kg	Tap water {Europe without Switzerland} | market for | Cut-off, U
Retarder powder	1	kg	Citric acid {GLO} | market for | Cut-off, U
Admixtures	1	kg	Plasticiser, for concrete, based on sulfonated melamine formaldehyde {GLO} | market for | Cut-off, U
Sand 0/2 mm	1	kg	Sand {RoW} | market for sand | Cut-off, U

The MK process is based on previous research [30] utilizing the kaolin clay process and incorporating additional energy required for the firing of MK.

Owing to the slightly different densities of the resulting materials, it is necessary for a more accurate calculation of the life cycle to recalculate the actual consumption of components per cubic meter of each composition. The recalculated mix compositions are summarized in Table 3.

Table 3. Experimental mix compositions (kg of raw components for 1 m^3 of fresh mix).

Mix No.:	PC Mortar	GCP1	GCP2	GCP3	GCP4	GCP5
Baugips Knauf (BG)		533	247			
Recycled gypsum (RG)			247	461		236
Phosphogypsum (PG)					512	236
CEM I 42.5 N	550	218	202	189	209	193
Metakaolin (MK)		218	202	189	209	193
Limestone filler	367					
Water	275	441	480	517	489	516
Admixture Plastretard		4.8	4.5	4.2	4.7	4.3
Complex admixture	18					
Sand 0/2 mm	899	485	449	420	466	430

3. Results and Discussion

3.1. Hardened Properties

The physical and mechanical properties of the materials tested are presented in Figures 4–8. Results for bulk density indicate that the GCP compositions possess a dry density below 1700 kg/m^3. This value is at least 200 kg/m^3 lower than that of compositions based on PC, which can be attributed to the lower density of the gypsum binder compared to the PC binder and the higher sand content in the PC mixture. For all compositions, the difference between wet and dry density ranges from 190 to 250 kg/m^3. This amount of water, which evaporates during the drying process, corresponds to the volume of free capillary pores that become empty after the free water evaporates (up to 25 vol.%). The differences in density can be explained by variations in microstructural packing determined by the particle size and microstructure of the gypsum component and different water–binder ratios. As a result, materials with varying porosity and structure are formed. For

example, RG is characterized by a porous grain structure (Figure 2) and the finest particle size distribution, resulting in the lowest density of composition GCP3. Composition GCP4, which is based on a PG gypsum source, provided slightly higher wet density compared to other compositions, while dry density was similar for all GCP compositions. This could be associated with the fineness of the PG binder and the attrition of extra water during the preparation of the 3D printable mixture.

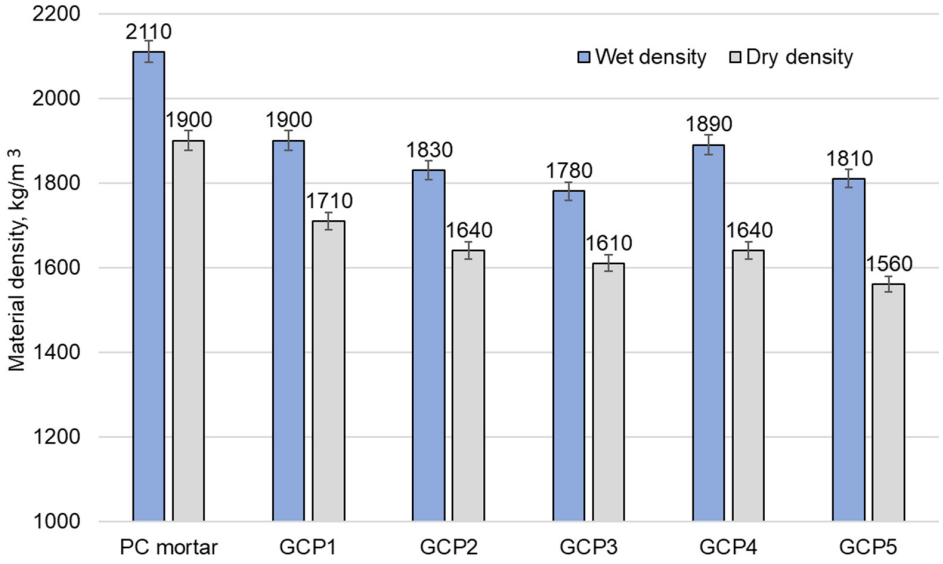

Figure 4. Material density in wet and dry conditions.

The results of the mechanical tests for the samples are displayed in Figure 5. Strength results demonstrate that at the age of 7 days, the GCP compositions achieve 70 to 85% of the 28-day strength, which is also comparable to the PC-based composition. It should be noted that the hardening mechanisms of GCP binders are still insufficiently studied. Most sources indicate that hardening occurs due to the hydration of cement minerals and the formation of calcium hydrosilicates, similar to the PC-based composition. Therefore, at an early age, the strength of the GCP composition is determined by the hydration of gypsum hemihydrate and the formation of ettringites, while further strength gain is determined by the formation of CSH gel during the hydration of PC minerals.

The experimental results correspond to those obtained in other studies, for instance, one study [10] recorded a 28-day compressive strength of 35 MPa for ternary calcium sulfate–GGBS–PC binders and about 20 MPa at the age of 7 days. Another research study [43] elaborated on gypsum–PC–mineral powder composites using flue gas desulfurization gypsum (FGD gypsum), achieving a strength of 24.7 MPa at the age of 28 days and a corresponding softening coefficient of 0.65, which is lower than those obtained in this research [42]. Generally, the strength of GCP compositions is not inferior to the strength of the PC compositions, and there is potential to expand the use of GCP compositions.

One of the most common and easily tested properties that determine the durability of a material is water absorption and the softening coefficient, which shows the reaction of the composite to long-term exposure to a humid environment. The water absorption and softening coefficient diagrams are shown in Figures 6 and 7, respectively.

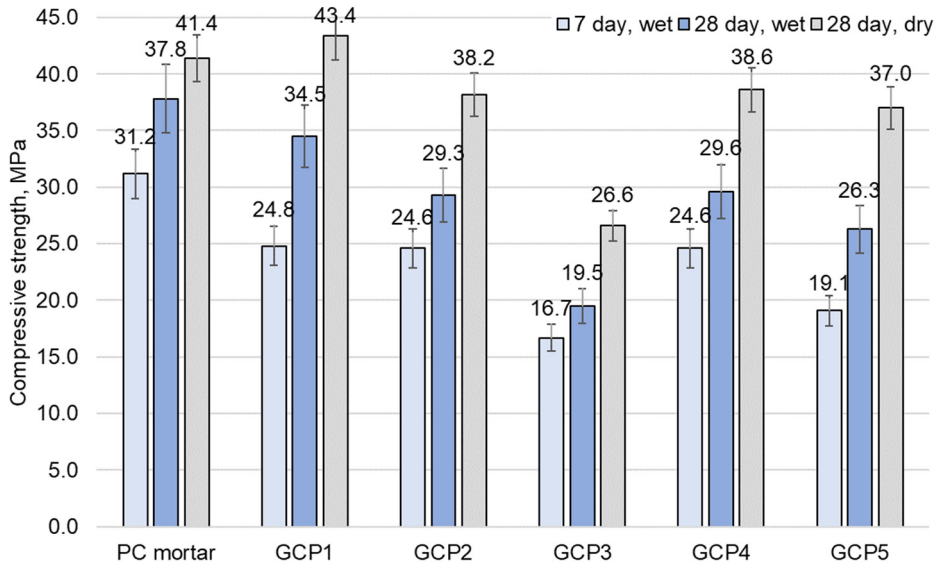

Figure 5. Compressive strength results.

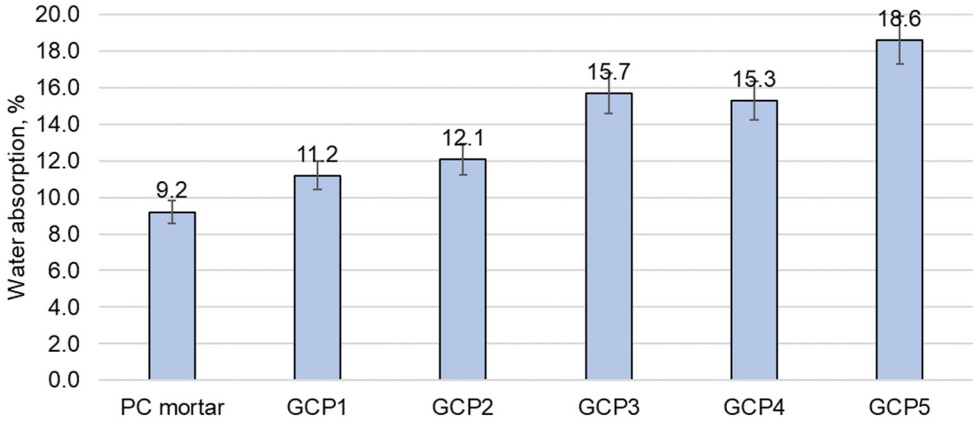

Figure 6. Water absorption values.

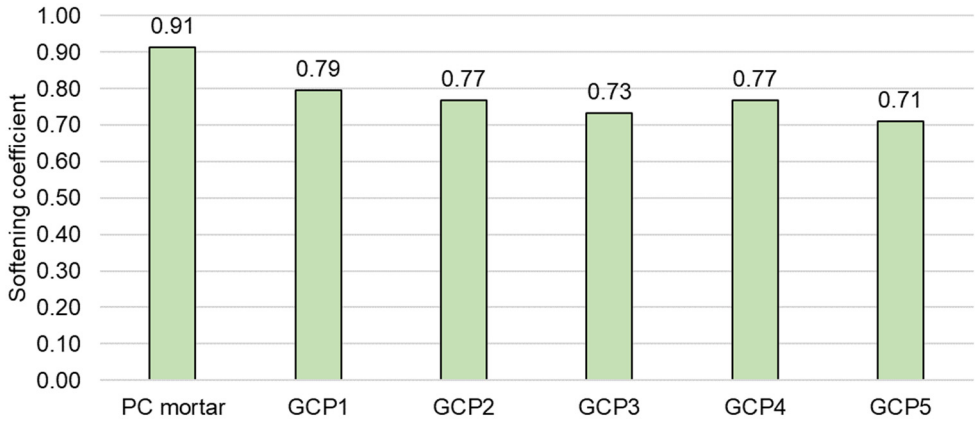

Figure 7. Softening coefficient values.

(**a**) (**b**)

Figure 8. Printed objects using GCP1 mixture: (**a**) side of square-shaped object; (**b**) straight thin wall.

Assessing the results of water absorption of samples (Figure 6), it is evident that GCP compositions exhibit higher water absorption values compared to the PC composition. The compositions based on RG, PG, and their combination with RG show the highest water absorption values, above 15%. This effect can be explained by the fact that these compositions are looser and contain an increased number of capillary voids due to a higher water–gypsum ratio. The lowest water absorption values (11–12%) were recorded for the pure-BG-based composition GCP1 and the BG combination with RG (GCP2). Data obtained by other researchers also indicate that the water absorption of GCP mixtures is higher than that of PC mixtures and ranges from 15 to 31% [43]. In [44], water absorption values from 5.9 to 10.4% were obtained.

The obtained softening coefficients of various GCP mixtures vary from 0.71 to 0.81 (Figure 7). These values significantly exceed the softening coefficients of pure gypsum but are slightly lower than the mixture based on PC. In this study, the softening coefficient for PC mortar was 0.91. The research by Gou et al. [43] developed optimal GCP compositions using the simplex-centroid design method. The best composition was characterized by a compressive strength of 25 MPa and a softening coefficient of 0.71 at 28 days. The value of the softening coefficient was the same, but the compressive strength was lower than those achieved in this research. The researchers [44] investigated the resistance of GCP mixes against the influence of water. It was found that after a short-term 2-day impact of water, the compositions exhibited softening coefficients greater than 0.91; however, there was a significant decrease in the strength and partial degradation of samples during long-term exposure to water. In the case of this research, the samples were kept in humid conditions for 28 days.

3.2. Three-Dimensional Printing

The consistency of each composite was evaluated at 5, 15, and 25 min after water was added to the dry mixture, as shown in Table 4. The flow diameter was maintained between 180 and 150 mm at the beginning of the 3D printing, which falls within the accepted printability range for the 3D extrusion printer used in this study. The results indicated that all mixtures were printable immediately after mixing, and the consistency remained relatively stable even after 25 min, providing a sufficient open printing time. A gradual decrease in flow diameter was detected, indicating processes associated with the crystallization and setting of the GCP mixtures. The workability reduction was much

more notable for the GCP mixture compared to the PC mortar mixture, which remained the same from 185 to 187 mm up to 25 min open time.

Table 4. Flow diameter (mm) of the used composites.

Mixture	PC Mortar	GCP1	GCP2	GCP3	GCP4	GCP5
5 min	187	157	157	162	162	181
15 min	185	156	151	160	153	180
25 min	185	156	146	158	149	179

Based on the results obtained, it was determined that mixture GCP1 exhibited the highest compressive strength, adequate durability properties, and suitable fresh characteristics for 3D printing, identifying it as having a potential application in construction. Consequently, this blend was selected for a 3D printing trial to evaluate its buildability and homogeneity during the process (Figure 8).

After printing 35 layers, more than initially anticipated, no collapse of the objects occurred, indicating satisfactory buildability. The dimensions of the straight wall and a square-shaped object were 500 mm and 200 × 200 mm, 350 mm high. Both objects were printed simultaneously with a layer interval time of 26 s. The total printing time for both objects was around 20 min, demonstrating good buildability owing to the mixture's relatively quick setting time. Although the print quality was deemed acceptable and the mixture was homogeneous, minor surface tearing and dimensional irregularities were observed, suggesting potential enhancements through adjustments to extrusion parameters, as shown in Figure 8a.

Other authors have conducted similar suitability assessments for 3D printing by performing flow table tests according to EN 1015-3 and subsequently assessing buildability through 3D printing [45,46]. These tests were conducted on PC mortars containing fly ash and silica fume. In one study, a printed object with geometry similar to the one presented here, using a mixture with a flow diameter of 150 mm, achieved a maximum height of 330 mm [45], consistent with the test findings in this research. In another case, a mixture with a similar flow diameter reached a print object height of 990 mm [36]. However, in this case, the layer width was significantly wider than in this research, resulting in reduced vertical stress and thereby explaining the enhanced buildability.

In both cases, when comparing the flow diameter and maximum print height values, it was observed that the mixtures with the most stable buildability exhibited flow diameter values in the range of 145–165 mm. From the mini cone test results obtained in this study, it is evident that the consistencies of all the developed GCP mixtures are similar to one another and comparable to the values from other studies that are recognized as suitable for 3D printing. Therefore, if the decision is made to 3D-print any of these mixtures, it is expected that their buildability will also be satisfactory.

The potential to enhance the buildability of the used mixtures is proposed. Currently, the materials are used in combination with a setting retarder for experimental purposes to prevent the mixture from setting too quickly. Conversely, if a decision was made to work without a retarder and the material was simultaneously mixed, pumped, and printed, the height of the print object could be infinite or constrained by the allowed print region dimensions, which are dependent on printer frame settings rather than material properties.

3.3. Life Cycle Assessment

In this study, the functional unit for the Life Cycle Assessment (LCA) is one cubic meter of material. This implies that the impact is determined by two factors: first, the amount of material required to produce one cubic meter and, second, the impact of these materials. Although the cement–metakaolin–gypsum ratio was the same for all GCP compositions, the use of different types of gypsum and their combinations resulted in different densities. This means that the amount of materials used per cubic meter also varies. This is the first factor that dictates the overall impact. The second factor is the impact of the raw materials.

The impact of cement and metakaolin as individual materials remains unchanged, but their proportional impact varies depending on the quantity used per cubic meter. In the case of different gypsums, this impact varies: BG has the full impact on the entire gypsum production cycle. RG uses recycled gypsum, so it does not have an impact on the raw material extraction stage. PG is used as waste material directly from the production line, so it has no impact on the production process, but this means that in the case of logistics, the printing itself must also be conducted near the production line.

Examining all the gypsum composite formulations, it can be seen that GCP1 has the highest impact, 380 kg CO_2 eq., mainly because this formulation uses only BG, which has the highest impact from gypsum. GCP2 has a slightly lower impact, 333 kg CO_2 eq., because only half of the composition is BG, the other half is RG, and overall, it has a lower density, thus also reducing the impact from cement compared to GCP1. The composition GCP3, which uses only RG, is shown as the binder with the least impact, producing 293 kg CO_2 eq., as displayed in Figure 9. This is due to the combination of low emissions from only using RG and a low density. Although GCP4 uses only PG, which has no emissions from production, its higher density means that there is more cement and MK in its composition, resulting in higher overall emissions, 318 kg CO_2 eq. GCP5, which uses both RG and PG, has emissions quite similar to GCP4, 296 kg CO_2 eq., because both of the gypsum raw materials used have low CO_2 emissions and also have a low density.

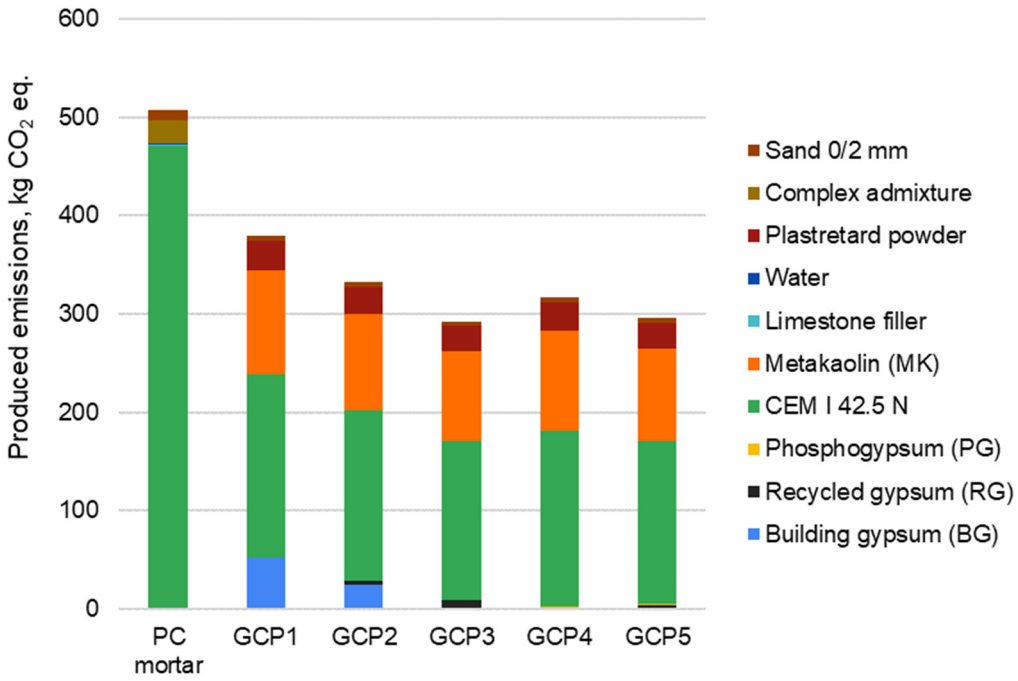

Figure 9. Produced greenhouse gas emissions for evaluated 3D printable mixture compositions.

A PC mortar with similar properties is shown to produce 508 kg CO_2 eq., which, compared to the GCP binders developed in this study, results in a higher environmental impact, with most of the impact coming from the cement. Compared to LCA results for 1 ton of LC^3, which is a new type of low-CO_2-emission blended cement that consists of MK, gypsum, limestone, and PC [46], where results vary from 350 to ~500 kg CO_2 eq., the results from this LCA are similar, yet lower. However, in this case, only stage A1 was considered, whereas for LC^3, stages A1–A3 were included; thus, the results should be higher.

Additionally, it should be noted that the study used CEM I cement, which has the highest emissions among all cement types and will be replaced by other types of cement in the near future. However, since these other cement types contain a large amount of SCMs, they interfere with determining the precise interactions between gypsum, cement, and pozzolan. Therefore, CEM I was specifically used in this study. If a different type of cement

were used, the overall results of all mixtures would show a lower CO_2 impact, yet the overall trend would remain that GCP composites can achieve significantly lower emissions.

It should be noted that very few publications are devoted to assessing the life cycle of ternary binder materials, particularly GCP compositions. In study [11], data on the LCA and carbon dioxide emissions for ternary blended mixtures based on PG were provided, and comparisons with PC mortar were made. It was found that when using alternative binders, up to 30% of energy can be saved, and CO_2 emissions can be reduced by up to 57%, which exceeds the reductions observed in the current study but is heavily dependent on the reference binder.

A comprehensive LCA of GCP composites reveals various results, as shown in Figure 10. Considering that the results in LCA impact categories are in different values and units, the results are shown based on impact weight—material with the highest impact has an impact of 100%, and other materials have 0–100% compared to the material with the highest impact. Thus, this allows us to determine the material with the least and biggest impact among the materials analyzed in this research. Only two additional categories—Ozone Formation for Human Health and Terrestrial Ecosystems—record the highest values in PC mortar among all six materials assessed. Interestingly, PC mortar also records the lowest impact in some other categories. Despite this variation, the primary focus of the developed materials remains on reducing global warming impacts, notably GHG emissions, where PC mortar clearly has the most significant effect. However, this assessment highlights that a material's high impact in one category does not necessarily predict similar results in others.

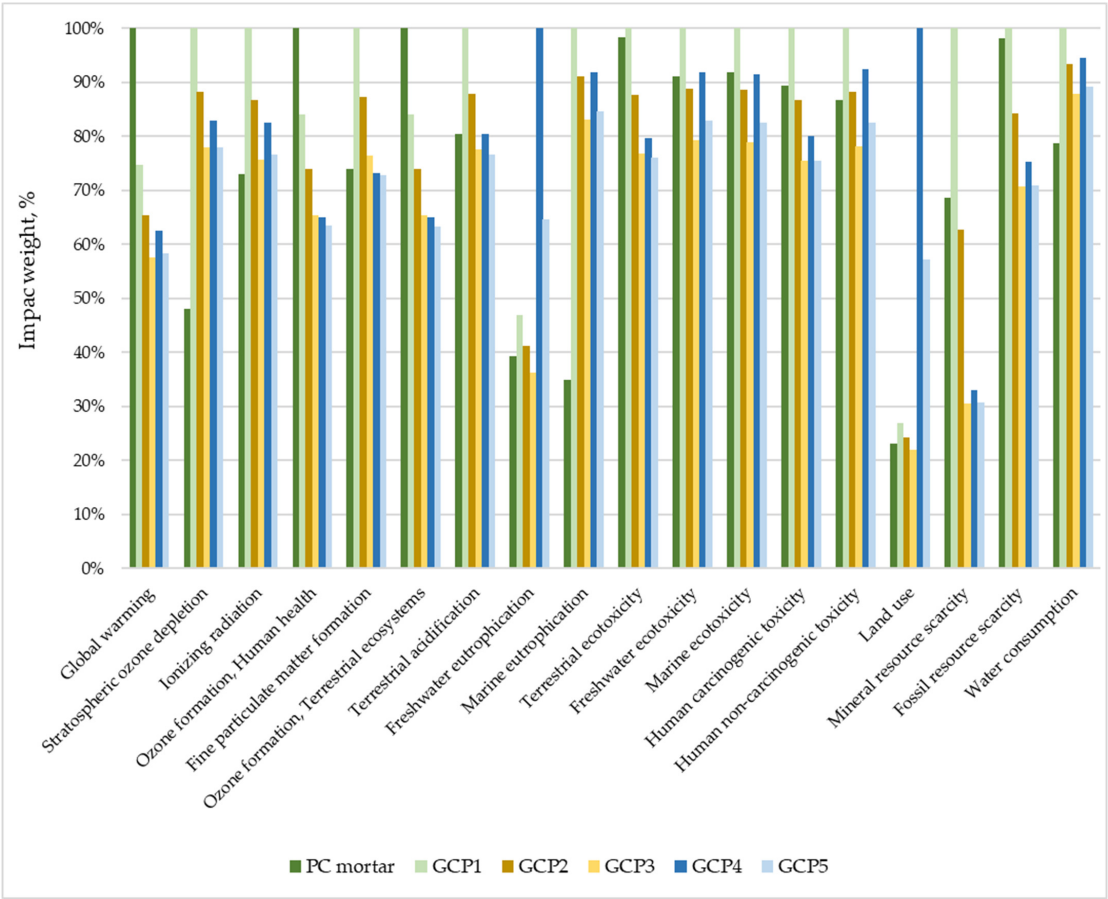

Figure 10. *Cont.*

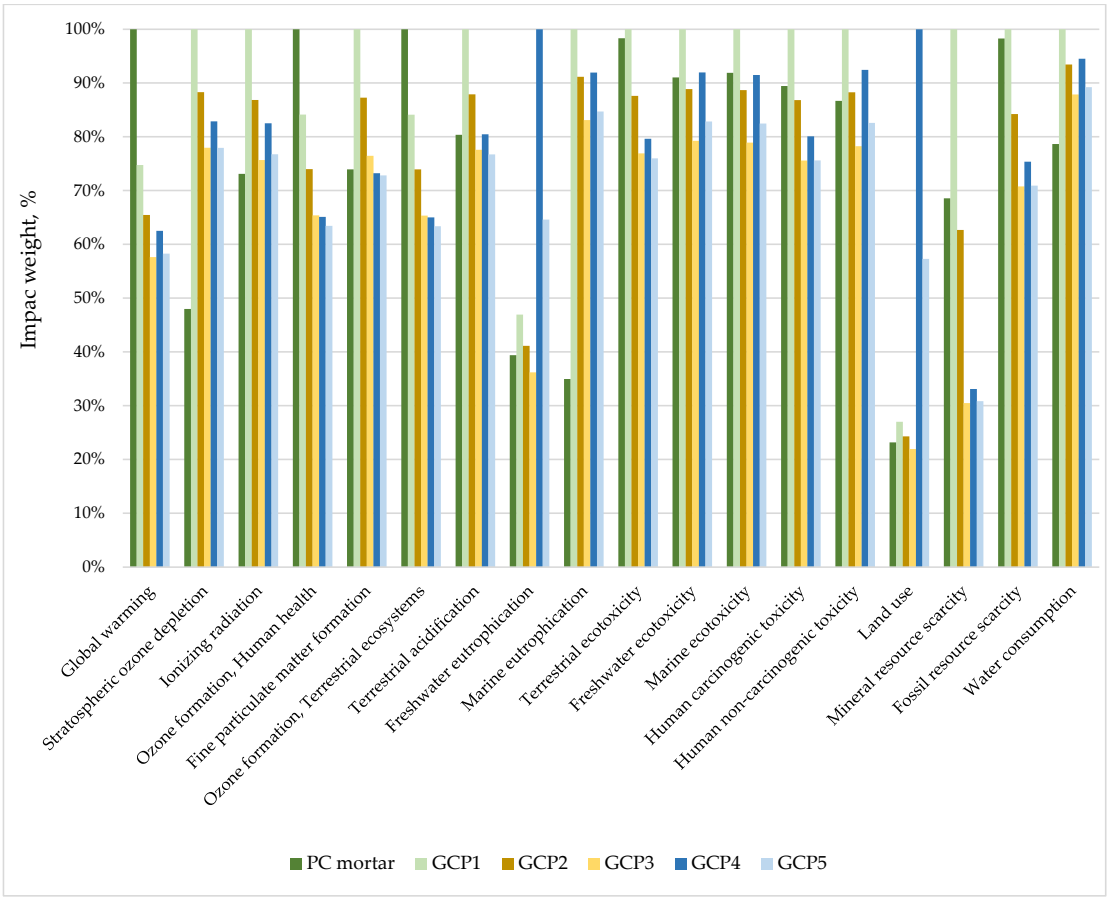

Figure 10. Life cycle assessment for PC mortar and five GCP binders.

When all impacts in LCA are considered, there are two fixed materials with the least impact, GCP3 and GCP5, but not in all impact categories. Therefore, when developing new materials, it is crucial to define the objective and focus on that, as different impact categories can yield varying results. Here, the results of the other GCP mixtures vary more than in the GWP category, as in some categories the variance can reach 75%. In other categories, raw materials play a more significant role; thus, different gypsum manufacturing methods contribute differently.

4. Conclusions

In this study, gypsum–cement–pozzolan (GCP) ternary system binder with various gypsum sources was used to develop material suitable for 3D printing. In general, all gypsum sources proved to be suitable for the development of GCP:

- GCP compositions have a minimum compressive strength of 30 MPa but lower water resistance than PC mortar. The softening coefficient ranged from 0.71 to 0.75, below PC mortar's 0.91.
- Tests show that natural gypsum can be partially replaced by recycled or artificial gypsum, with a potential strength reduction of up to 15%. Low-temperature-treated recycled gypsum is still viable for GCP production. A recycling system and industrial technology for gypsum board processing and thermal treatment are essential. The positive aspect is that gypsum heat treatment requires only 140 °C, low energy, and emits no CO_2.
- LCAs for GCP highlight a positive shift toward sustainable material production. GCP3 has the lowest and PC mortar the highest impact in the scope of CO_2 emissions. Examining various environmental impacts is crucial, as materials with low GHG emissions may affect other environmental categories like land use or water, e.g., the

GCP3 composite scored higher in ozone depletion and marine eutrophication than the PC mixture.
- Using GCP compositions can cut the carbon footprint by up to 40% compared to PC-based compositions, with the potential for greater reductions through further optimization of GCP mixtures and the binder–filler ratio.

Author Contributions: Conceptualization, G.S., G.B., M.S. and D.B.; methodology, G.S., A.S., G.B. and M.S.; software, L.P. and M.S.; validation, G.S., G.B. and M.S.; formal analysis, G.S., L.P., A.S., P.S. and M.S.; investigation, G.S., L.P., A.S. and P.S.; resources, G.S. and D.B.; data curation, G.S., A.S. and G.B.; writing—original draft preparation, G.S., L.P. and A.S.; writing—review and editing, A.S., P.S., G.B. and M.S.; visualization, G.S., A.S., P.S. and M.S.; supervision, G.B., M.S. and D.B.; project administration, G.S., M.S. and D.B.; funding acquisition, G.S. and D.B. All authors have read and agreed to the published version of the manuscript.

Funding: This research is funded by the FLPP (Fundamental and Applied Research Projects) Program in Latvia under the research project lzp-2022/1-0585 "Development and characterization of sustainable gypsum–cement–pozzolanic ternary compositions for 3D printing".

Data Availability Statement: The original contributions presented in the study are included in the article, further inquiries can be directed to the corresponding author.

Conflicts of Interest: The authors declare no conflicts of interest.

References

1. Manjunatha, M.; Preethi, S.; Malingaraya; Mounika, H.G.; Niveditha, K.N. Ravi Life Cycle Assessment (LCA) of Concrete Prepared with Sustainable Cement-Based Materials. *Mater. Today Proc.* **2021**, *47*, 3637–3644. [CrossRef]
2. Snellings, R.; Suraneni, P.; Skibsted, J. Future and Emerging Supplementary Cementitious Materials. *Cem. Concr. Res.* **2023**, *171*, 107199. [CrossRef]
3. Bumanis, G.; Vitola, L.; Pundiene, I.; Sinka, M.; Bajare, D. Gypsum, Geopolymers, and Starch-Alternative Binders for Bio-Based Building Materials: A Review and Life-Cycle Assessment. *Sustainability* **2020**, *12*, 5666. [CrossRef]
4. Fo, J.; Cerný, R. Carbon Footprint Analysis of Calcined Gypsum Production in the Czech Republic. *J. Clean. Prod.* **2018**, *177*, 795–802. [CrossRef]
5. Potapova, E.; Guseva, T.; Shchelchkov, K. Mortar for 3D Printing Based on Gypsum Binders Mortar for 3D Printing Based on Gypsum Binders. *Mater. Sci. Forum* **2021**, *1037*, 26–31. [CrossRef]
6. Pan, H.; Wu, X.; Song, K.; Zhang, Y.; Zhao, Q. Preparation of Calcium Sulphoaluminate Cement-Portland Cement-Gypsum Based Sleeve Grouting Material: Performance Optimization and Tensile Properties of Sleeve Connector. *Constr. Build. Mater.* **2024**, *418*, 135341. [CrossRef]
7. Calderón-Morales, B.R.S.; García-Martínez, A.; Pineda, P.; García-Tenório, R. Valorization of Phosphogypsum in Cement-Based Materials: Limits and Potential in Eco-Efficient Construction. *J. Build. Eng.* **2021**, *44*, 102506. [CrossRef]
8. Çolak, A. Physical, Mechanical, and Durability Properties of Gypsum–Portland Cement–natural Pozzolan Blends. *Can. J. Civ. Eng.* **2001**, *28*, 375–382. [CrossRef]
9. Bumanis, G.; Zorica, J.; Bajare, D. Properties of Foamed Lightweight High-Performance Phosphogypsum-Based Ternary System Binder. *Appl. Sci.* **2020**, *10*, 6222. [CrossRef]
10. Rourke, B.O.; Mcnally, C.; Richardson, M.G. Development of Calcium Sulfate–Ggbs–Portland Cement Binders. *Constr. Build. Mater.* **2009**, *23*, 340–346. [CrossRef]
11. Bumanis, G.; Korjakins, A.; Bajare, D. Environmental Benefit of Alternative Binders in Construction Industry: Life Cycle Assessment. *Environments* **2022**, *9*, 6. [CrossRef]
12. Bumanis, G.; Zorica, J.; Korjakins, A.; Bajare, D. Processing of Gypsum Construction and Demolition Waste and Properties of Secondary Gypsum Binder. *Recycling* **2022**, *7*, 30. [CrossRef]
13. Nizevičienė, D.; Vaičiukynienė, D.; Michalik, B.; Bonczyk, M.; Vaitkevičius, V.; Jusas, V. The Treatment of Phosphogypsum with Zeolite to Use It in Binding Material. *Constr. Build. Mater.* **2018**, *180*, 134–142. [CrossRef]
14. Cao, C.; Sun, D.; Xian, Z.; Zhang, H. A Brief Review of 3D Printed Concrete. *Highlights Sci. Eng. Technol.* **2022**, *28*, 374–380. [CrossRef]
15. Struct, J.C.; Jo, J.H.; Jo, B.W.; Cho, W.; Kim, J.H. Development of a 3D Printer for Concrete Structures: Laboratory Testing of Cementitious Materials. *Int. J. Concr. Struct. Mater.* **2020**, *14*, 13. [CrossRef]
16. Ghosh, D. TRACE: Tennessee Research and Creative Exchange A Study on Early Age Properties of Concrete for Precast and 3D Printing. Ph.D. Thesis, University of Tennessee, Knoxville, TN, USA, 2022.
17. Shafighfard, T.; Cender, T.A.; Demir, E. Additive Manufacturing of Compliance Optimized Variable Stiffness Composites through Short Fiber Alignment along Curvilinear Paths. *Addit. Manuf.* **2021**, *37*, 101728. [CrossRef]

18. Zhang, Y.; Zhang, Y.; She, W.; Yang, L.; Liu, G.; Yang, Y. Rheological and Harden Properties of the High-Thixotropy 3D Printing Concrete. *Constr. Build. Mater.* **2019**, *201*, 278–285. [CrossRef]
19. Zaid, O.; El Ouni, M.H. Advancements in 3D Printing of Cementitious Materials: A Review of Mineral Additives, Properties, and Systematic Developments. *Constr. Build. Mater.* **2024**, *427*, 136254. [CrossRef]
20. Shakor, P.; Nejadi, S.; Paul, G.; Sanjayan, J. Dimensional Accuracy, Flowability, Wettability, and Porosity in Inkjet 3DP for Gypsum and Cement Mortar Materials. *Autom. Constr.* **2020**, *110*, 102964. [CrossRef]
21. Zhou, S.; Lu, Y.; Pan, Y.; Li, J.; Qu, F.; Luo, Z.; Li, W. Flowability Prediction of Recycled α-Hemihydrate Gypsum for 3D Powder Printing under Combined Effects of Different Glidants Using Response Surface Methodology. *Dev. Built Environ.* **2023**, *16*, 100265. [CrossRef]
22. Ma, X.; Tan, L.; Lu, Y.; Yao, W.; Wei, Y. Upcycling of Waste Plasterboard for the Synthesis of High-Quality Gypsum-Based 3D Printing Powder. *Constr. Build. Mater.* **2023**, *373*, 130846. [CrossRef]
23. Ma, B.; Lu, W.; Su, Y.; Li, Y.; Gao, C.; He, X. Synthesis of α-Hemihydrate Gypsum from Cleaner Phosphogypsum. *J. Clean. Prod.* **2018**, *195*, 396–405. [CrossRef]
24. Lu, W.; Ma, B.; Su, Y.; He, X.; Jin, Z.; Qi, H. Preparation of α-Hemihydrate Gypsum from Phosphogypsum in Recycling $CaCl_2$ Solution. *Constr. Build. Mater.* **2019**, *214*, 399–412. [CrossRef]
25. Zhang, L.; Mo, K.H.; Tan, T.H.; Hung, C.-C.; Yap, S.P.; Ling, T.-C. Influence of Calcination and GGBS Addition in Preparing β-Hemihydrate Synthetic Gypsum from Phosphogypsum. *Case Stud. Constr. Mater.* **2023**, *19*, e02259. [CrossRef]
26. Jin, Z.; Ma, B.; Su, Y.; Lu, W.; Qi, H.; Hu, P. Effect of Calcium Sulphoaluminate Cement on Mechanical Strength and Waterproof Properties of Beta-Hemihydrate Phosphogypsum. *Constr. Build. Mater.* **2020**, *242*, 118198. [CrossRef]
27. Rodrigo-Bravo, A.; Alameda Cuenca-Romero, L.; Calderon, V.; Rodriguez, A.; Gutiérrez-González, S. Comparative Life Cycle Assessment (LCA) between Standard Gypsum Ceiling Tile and Polyurethane Gypsum Ceiling Tile. *Energy Build.* **2022**, *259*, 111867. [CrossRef]
28. Pedreño-Rojas, M.A.; Fořt, J.; Černý, R.; Rubio-de-Hita, P. Life Cycle Assessment of Natural and Recycled Gypsum Production in the Spanish Context. *J. Clean. Prod.* **2020**, *253*, 120056. [CrossRef]
29. Genc, G.; Demircan, R.K.; Beyhan, F.; Kaplan, G. Assessment of the Sustainability and Producibility of Adobe Constructions Reinforced with Ca-Based Binders: Environmental Life Cycle Analysis (LCA) and 3D Printability. *Sci. Total Environ.* **2024**, *906*, 167695. [CrossRef]
30. Scheinherrová, L.; Doleželová, M.; Vimmrová, A.; Vejmelková, E.; Jerman, M.; Pommer, V.; Černý, R. Fired Clay Brick Waste as Low Cost and Eco-Friendly Pozzolana Active Filler in Gypsum-Based Binders. *J. Clean. Prod.* **2022**, *368*, 133142. [CrossRef]
31. Suárez, S.; Roca, X.; Gasso, S. Product-Specific Life Cycle Assessment of Recycled Gypsum as a Replacement for Natural Gypsum in Ordinary Portland Cement: Application to the Spanish Context. *J. Clean. Prod.* **2016**, *117*, 150–159. [CrossRef]
32. *EN 197-1*; Cement—Part 1: Composition, Specifications and Conformity Criteria for Common Cements. European Committee for Standardization: Brussels, Belgium, 2011.
33. *EN 13279-1*; Gypsum Binders and Gypsum Plasters—Part 1: Definitions and Requirements. European Committee for Standardization: Brussels, Belgium, 2008.
34. *EN 196-1*; Methods of Testing Cement—Part 1: Determination of Strength. European Committee for Standardization: Brussels, Belgium, 2016.
35. *EN 1015-3*; Methods of Test for Mortar for Masonry—Part 3: Determination of Consistence of Fresh Mortar (by Flow Table). European Committee for Standardization: Brussels, Belgium, 1999.
36. Ivanova, I.; Ivaniuk, E.; Bisetti, S.; Nerella, V.N.; Mechtcherine, V. Comparison between Methods for Indirect Assessment of Buildability in Fresh 3D Printed Mortar and Concrete. *Cem. Concr. Res.* **2022**, *156*, 106764. [CrossRef]
37. Roussel, N.; Coussot, P. "Fifty-Cent Rheometer" for Yield Stress Measurements: From Slump to Spreading Flow. *J. Rheol.* **2005**, *49*, 705–718. [CrossRef]
38. Bos, F.P.; Kruger, P.J.; Lucas, S.S.; van Zijl, G.P.A.G. Juxtaposing Fresh Material Characterisation Methods for Buildability Assessment of 3D Printable Cementitious Mortars. *Cem. Concr. Compos.* **2021**, *120*, 104024. [CrossRef]
39. *ISO/ASTM 52939*; Additive Manufacturing for Construction—Qualification Principles—Structural and Infrastructure Elements. ISO: Geneva, Switzerland, 2023.
40. Kruger, J.; Zeranka, S.; van Zijl, G. 3D Concrete Printing: A Lower Bound Analytical Model for Buildability Performance Quantification. *Autom. Constr.* **2019**, *106*, 102904. [CrossRef]
41. Spurina, E.; Sinka, M.; Ziemelis, K.; Vanags, A.; Bajare, D. The Effects of Air-Entraining Agent on Fresh and Hardened Properties of 3D Concrete. *J. Compos. Sci.* **2022**, *6*, 281. [CrossRef]
42. Tsioka, M.; Voudrias, E.A. Comparison of Alternative Management Methods for Phosphogypsum Waste Using Life Cycle Analysis. *J. Clean. Prod.* **2020**, *266*, 121386. [CrossRef]
43. Gou, M.; Zhao, M.; Zhou, L.; Zhao, J.; Hou, W.; Ma, W. Hydration and Mechanical Properties of FGD Gypsum-Cement- Mineral Powder Composites. *J. Build. Eng.* **2023**, *69*, 106288. [CrossRef]
44. Gaidučis, S.; Žvironaitė, J. Resistance of Phosphogypsum Cement Pozzolanic Compositions against the Influence of Water. *Mater. Sci.* **2011**, *17*, 308–313. [CrossRef]

45. Cho, S.; Kruger, J.; Bester, F.; van den Heever, M.; van Rooyen, A.; van Zijl, G. *A Compendious Rheo-Mechanical Test for Printability Assessment of 3D Printable Concrete*; Springer: Berlin/Heidelberg, Germany, 2020; pp. 196–205.
46. Arruda Junior, E.S.; de Sales Braga, N.T.; Barata, M.S. Life Cycle Assessment to Produce LC^3 Cements with Kaolinitic Waste from the Amazon Region, Brazil. *Case Stud. Constr. Mater.* **2023**, *18*, e01729. [CrossRef]